Harmonizing Dynamic Property Measurements of Hungarian Soils

R.P. Ray
Department of Structural and Geotechnical Engineering, Széchenzi István University, Győr, Hungary, ray@sze.hu

Akos Wolf, Orsolya Kegyes-Brassai
Department of Structural and Geotechnical Engineering, Széchenzi István University, Győr, Hungary, wolf@sze.hu , kegyesbo@sze.hu

ABSTRACT: With the adoption of EC-8, geotechnical engineers in Hungary found themselves on unfamiliar ground. Previous codes required little in the way of dynamic properties (v_s, G_{max}, G_{red}, D) and seismic assessments were performed for critical sites only (nuclear power). The new code required new assessment methodologies, new measurements, new analyses, and new cooperation with structural engineers and architects. This presentation will illustrate some of the challenges in harmonizing various field and laboratory tests, as well as their use in design and analysis. Studies at Széchenyi University, as well as work with geotechnical consultants, attempted to maximize the usefulness of field, laboratory and performance data to generate a holistic, consistent set of dynamic properties of several categories of Hungarian soils. The effort has resulted in a robust, reliable set of properties and correlations which will serve as a basis for future research, design and construction.

Keywords: soil dynamics; field seismic testing; site response; field correlations

1. Introduction

The adoption of Eurocode has placed more emphasis on considering seismic actions, even for regions with moderate seismicity. Previous Hungarian codes had used static lateral loading to simulate seismic contributions. With the newer requirements, such an approach was no longer possible. The design methods could be brought into the state of practice through training programs, short courses and adjustments to university curricula. More difficult perhaps was the lack of baseline data on dynamic properties (v_s, G_{max}, G_{red}, D) of soils throughout Hungary. Similar challenges were faced by neighboring countries as well. This paper summarizes efforts to establish dynamic property data by in-situ methods, then embellish that data with laboratory testing and computer modeling. Since a holistic approach makes more sense than mere data gathering in the field, I will address all three with an emphasis on in-situ testing.

2. Motivation

Martin Sara [1] wrote an excellent Geoenvironmental Site Characterization handbook in 1994. In it he states:

The most important data is that which is used in making decisions, therefore, only collect data this is part of the decision-making process.

This concept requires a more holistic approach to testing. With every test (field or laboratory) the geotechnical engineer should ask "is this test helping me decide something?" Of course, the answer requires some knowledge of the entire project. Unfortunately, the answer to the question often arrives at the very end of the investigation when the engineer is writing a final report; too late to go back to investigate further.

Research projects may have more time and flexibility to allow for this approach. However, based on personal experience, unless there is a conscious decision during the planning stages of the research, such a luxury is often lost to inevitable deadlines and deliverables. In the following sections, I will describe some of the projects my colleagues and I have been working on to help illustrate the holistic concept. I will present some of the data we gathered and show how we put it to (hopefully) good use. Having worked in geotechnical engineering for 42 years, I can reassure the reader that there are still plenty of interesting challenges out in the field, in the lab, and on the computer monitor.

3. Squeezing data from a rock (or soil)

One of the first challenges we faced in our research was building a baseline of dynamic properties for Hungarian soils. Starting small, we studied dynamic properties of Hungarian soils common to Győr, where we wanted to perform a seismic risk assessment of the city. At the time, there were no profiles of shear wave velocity within the county. Comprehensive data on dynamic properties were focused on the Paks nuclear power plant; a distance of 150km, and well beyond the range even the most optimistic semi-variogram.

3.1. MASW in the city

With expert help from the Hungarian Institute of Geophysics we were able to perform a series of MASW tests at 11 locations around the city (Fig. 1) [2,3]. A number of surface wave methods have been proposed for near-surface characterization by using a great variety of testing configurations, processing techniques, and inversion algorithms. The MASW method [4] is regarded as the

most effective technique in urban environments, because multichannel records make it possible to separate different wave fields by applying 2D Fourier transform (in the frequency-wavenumber, ***f–k*** domain, [6]) or phase shift method (in the frequency-phase velocity, ***f–c*** domain, [7]) and making it less sensitive to environmental noise and coupling of receivers [8]. Data processing consisted of two main steps: (i) Obtaining the dispersion curves of Rayleigh wave phase velocity from the records and (ii) determining the v_s profiles. The processing was carried out by RadexPro software [9]. The records are first muted to reduce spectral leakage, the effect of random noise, and interference with other wave types. After muting, only the surface wave component (jumping up) of the SR–II (Fig. 2) is used for ***f–c*** transformation by phase shift method. The dispersion curve is obtained from the (absolute and relative) maxima of the ***f–c*** spectrum (Fig. 3). The ***f-k*** domain image gives a different viewpoint about the inherence of the linked plumes of maxima as shown in Fig. 3 which is very useful in delimiting dispersion curves.

Figure 1. Slight air gap between explosive source and soil medium

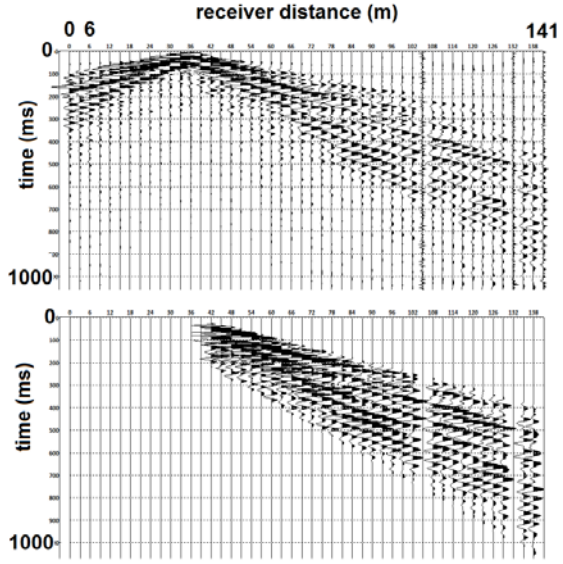

Figure 2. Seismic record before and after tapering

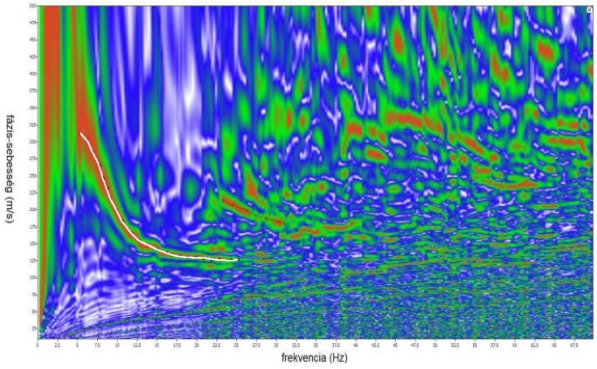

Figure 3. MASW Phase velocity vs. frequency dispersion image. The white trace is used to invert the profile.

The maximum depth of investigation is around 30m depending on site and source conditions and is dictated by the longest wavelength made by the impact source. Greater impact power translates to longer wavelengths and deeper sampling depths. Vertical low-frequency geophones (< 4.5 Hz) are recommended as receivers. The length of the receiver spread, usually limited to 50-100m, is directly related to longest wavelength detected while receiver spacing (distance between receivers) relates to the shortest wavelength detected. The source and receiver spread distance is one of the variables that affect the horizontal resolution of the dispersion curve [4].

3.2. Extending Correlations

There was no soil profile database for the city of Győr, however there were 60 drilling records from the North Transdanubian Environmental Protection and Water Management Inspectorate. We then proceeded to correlate the data from MASW tests to boring data. Since the boring data listed soil types and the extent of layering throughout the study area, MASW data was matched with nearby boring logs to determine if the v_s data could be correlated to local soil types. Most correlations have the form:

$$v_{s,i} = a D^b \tag{1}$$

where a can be interpreted as a basic v_s value for each soil category, D is depth, and b is the depth correlation coefficient. Using the 11 MASW profiles, we were able to match v_s with various soil types at different depths. Examples of three such correlations are shown in Fig. 3

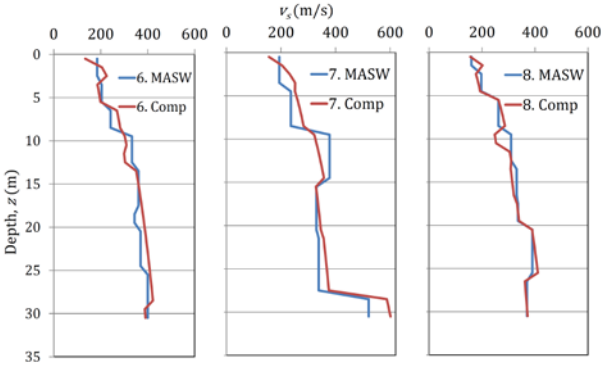

Figure 4. Profiles comparing curve fit and measured MASW data

So, the correlations allowed us to extend our data over the entire city area and develop better predictions of local

site amplification. This led to better decisions on seismic risk among different city districts.

4. Extending the CPT database

Hungarian geotechnical engineers have used CPT data in their designs for quite some time. They are comfortable with the test data and methods to apply that data for shallow and deep foundation design. Naturally, it was a logical decision to try and correlate this wealth of CPT data to v_s and apply it to site response evaluation, or at least to generate EC-8 soil profiles.

4.1. Four Correlations

For our analyses, correlation equations suggested by Hegazy and Mayne (H&M) [6], Andrus et al (A) [7], Robertson (R) [8] and Tonni and Simonini (T&S) [9] are discussed in the following sections.

Hegazy and Mayne [6] improved the relationship recommended in [10] based on more data for clay soils and showed that initial void ratio (e_0) and cone tip resistance (q_c) were significant parameters in the correlation. Considering that the void ratio is not known in all cases, another equation was proposed which was independent of e_0 and dependent only on cone data. For sand, q_c and effective vertical stress (σ_{v0}')are the most significant parameters while the sleeve friction (f_s) has less effect, based on simple and multiple analyses of data from 24 sand sites. Based on a very large database of all soil types a general correlation was proposed, which depends on only CPT results:

$$v_s = \left(10.1 \cdot \log q_c - 11.4 \right)^{1.67} \cdot \left(100 \cdot f_s / q_c \right)^{0.3} \quad (2)$$

Andrus et al. [7], for Holocene and Pleistocene soils, suggested the following equation based on regression analysis:

$$v_s = 2.62 \cdot q_t^{0.395} \cdot I_c^{0.912} \cdot D^{0.124} \cdot SF \quad (3)$$

where q_t (kPa) is the measured cone tip resistance corrected for pore pressure, I_c (-) is the soil type behavior index, D (m) is the depth below the ground surface, which denotes the overburden stress. Scaling factor (SF) represents the difference between the Holocene and Pleistocene soils; it is 0.92 for the younger deposit and 1.12 for older sediments. These values indicate that the v_s in Pleistocene deposits is 22-26% higher than v_s in Holocene deposits.

Robertson [8] also used the normalized parameters from CPT results and measured shear wave velocity [10]. He improved the previously recommended normalized tip resistance with:

$$v_s = \left(10^{0.55 \cdot I_c + 1.68} \cdot \left(q_t - \sigma_{v0} \right) / p_a \right)^{0.5} \quad (4)$$

where q_t is the cone tip resistance corrected for pore pressure, and σ_{v0} and σ_{v0}' are the total and effective overburden stress. The term p_a is the atmospheric pressure, and the exponent n can be calculated as a function of soil behavior type index I_c as,

$$n = 0.381 \cdot I_c + 0.05 \cdot \left(\sigma_{v0}' / p_a \right) - 0.15 \le 1.0 \quad (5a)$$

$$I_c = \left[\left(3.47 - \log Q \right)^2 + \left(\log F + 1.22 \right)^2 \right]^{0.5} \quad (5b)$$

$$Q = \left(q_t - \sigma_{v0} \right) / \sigma_{v0}' \quad (5c)$$

$$F = f_s / \left(q_t - \sigma_{v0} \right) \cdot 100 \quad (5d)$$

where f_s is sleeve friction. Equation 4 is recommended to estimate the shear wave velocity of most Holocene and Pleistocene age soils, but they may underestimate v_s in Pleistocene deposits.

For a location in Italy, despite the common mineralogical origin and the similar frictional based mechanical response, the predominantly sandy sediments follow a different trend compared to silts-silt mixtures and transitional soils [8]. From Eq.4, the constants were adjusted to fit the database for the Italian region, and the following equation was developed:

$$v_s = 10^{0.31 \cdot I_c + 0.77} \cdot \left(\left(q_t - \sigma_{v0} \right) / p_a \right)^{0.5} \quad (6)$$

All these equations represent a large number of soundings and shear wave velocity measurements. Many of the Hungarian soils were of similar geologic age.

5. Hungarian soils tested

For our research, CPT data with shear wave velocity profiles were collected for seven Hungarian locations: Budapest, Kaposvár, Komárom, Paks-1, Paks-2, Szolnok, and Tivadar [10]. For all locations, the soil strata were known, but more detailed data, such as index laboratory test results (plasticity index, grain size distribution) do not exist. Therefore, our research will focus only on CPT data with soil type behavior index used to estimate the soil type. The ground water level for the locations is also known and overburden stress was calculated assuming a unit weight γ = 19.5 kN/m^3.

In Hungary, 80% of the surface is covered by Quaternary deposits. The thickness is highly variable; in the hilly areas it is only 10-20 m, while in shallow basins it can be several hundreds of meters thick. Since most of the existing recommendations in the literature are based on similar Quaternary deposits, improving the correlation relations for these soils is possible.

5.1. Geologic grouping

From a geologic point of view, the locations can be divided into four groups:

a) Holocene fluvial deposit. Soft, thick profiles found in Tivadar and Szolnok (q_c = 1-2 MPa, $I_c \approx$ 3.0). Total data pairs = 32

b) Pleistocene fluvial deposit. Danube river deposits generally dense, coarse-grained located in Komárom, Budapest and Paks-2 (q_c = 15-40 MPa, I_c = 1-2). Total data pairs = 154
c) Pleistocene aeolian deposit. Loess and windblown sands. Kaposvár and Paks-1 (q_c = 1-5 MPa, I_c = 2.7-3.0, I_p = 10-13%). Total data pairs = 64
d) Tertiary deposit. Deeper formations in Budapest and Paks-2 (q_c = 7-13 MPa, I_c = 2.3-2.7). Total data pairs = 31

The geologic age has a definite influence on the q_c-v_s relationship as shown in Fig. 4.

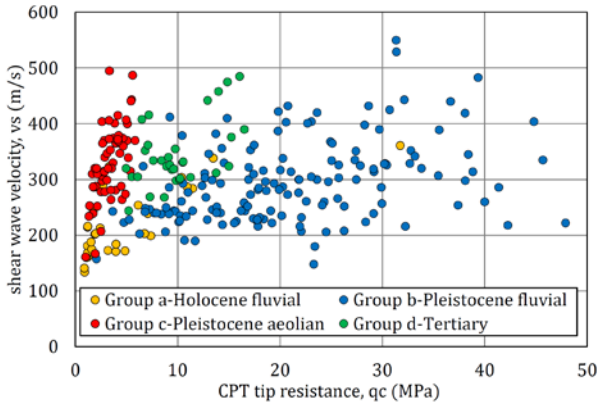

Figure 5. CPT q_u and v_s for four soil groups

5.2. Measurements and metrics

All shear wave velocities were measured by seismic CPT tests (SCPT). For SCPT, the cone is equipped with two geophones at a separation of 0.5 m. For the v_s measurement, the CPT cone is paused, then a shear wave is generated by striking the end of a beam that is pressed against the ground by the weight of the CPT vehicle [15]. Propagation time can be assessed based on first arrival of the waves or peak to peak method. The shear wave velocity can be obtained as

$$v_s = \Delta l \,/\, \Delta t \qquad (7)$$

where the Δl is the travel distance between the two geophones, generally 0.5 m, and Δt is the propagation time of waves. Based on this measurement method, v_s is valid for a 50 cm thick layer.

To better quantify the variability of CPT measurements over a given 0.5m interval, the maximum, minimum, mean (μ), standard deviation (sd), and relative standard deviation ($rsd=sd/\mu$) of q_c was computed. With 1 to 2-cm CPT intervals, 25-50 readings were analyzed for each v_s measurement.

In order to compare the accuracy of the predicition equations (Eq. 2,3,4,6), relative error (e_r) was computed for each method.

$$e_r = \left(v_{se} - v_{sm}\right) / v_{sm} \qquad (8)$$

where v_{se} is estimated and v_{sm} is measured shear wave velocity, respectively. A positive value means v_s is overestimated and a negative value, underestimated. The absolute value of relative error is also checked in some cases.

5.3. Data screening and grouping

There were other issues to be considered when building the database for correlation. These include eliminating questionable soils, interfaces with highly contrasting v_s values, and reconciling the different sampling intervals for CPT and v_s measurements.

Near-surface layers often consist of fill or organic soils. Additionally, the influence due to the horizontal offset from the exciter (beam) to the cone on the wave propagation is significant, therefore we analyzed only the data deeper than 3-4 m as done by other researchers [6,11].

Shear wave velocity values can be scattered if there is a layer interface or geologic age shift near or within the measurement zone. Researchers often removed shear wave velocity data from the database if the CPT data (q_c or f_s) change significantly in the defined layer. In our analyses, rsd was used to track the variability. In the first step, we unselected the v_s measurement interval if rsd was more than 0.5. Prediction equations were then applied to the remaining data and compared to measurements. The process was repeated using lower (more restrictive) values down to rsd=0.05.

The effect of rsd on the accuracy of the estimations is shown on the Fig. 5. The gold line shows the size of the resulting data set after the rsd criteria is applied. As the criteria becomes less restrictive, the number of data pairs increases.

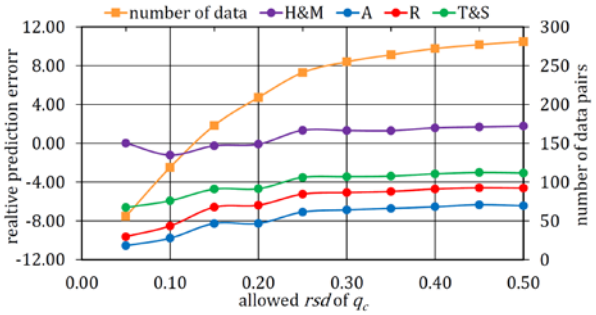

Figure 6. Effect of relative standard deviation on prediction error

Three of the four methods show a slight improvement in prediction with the inclusion of more data. However, the accuracy of H&M decreases with increasing rsd. Based on this examination we concluded that the rsd of q_c had no significant effect on the accuracy of estimations. Therefore, in the following comparison and improvement, all of data mentioned in section 5-1were analyzed. A total of 281 data pairs are available.

The v_s values measured by SCPT correspond to a "sampling" distance of 50 cm between the two geophones. However, CPT data is recorded at intervals of 1-2 cm therefore, for a 50-cm thick layer there are 25-50 CPT measured data. No information has been found in the previous publications how to reconcile the differences in sampling distance or how to average readings. There are three general ways to aggregate the CPT data to produce an estimate of the 50-cm interval:

1. Aggregate the raw CPT values (q_c, f_s) to single values for the interval.
2. Process the raw data individually to produce secondary data (I_c, D, SF, n, Q, F) then aggregate the secondary data to produce a single value and compute a single v_s
3. Process all raw and secondary data to produce v_s individually, then aggregate for the interval as a final step.

The aggregation process itself could be computing averages, weighted averages, or using an inverse weighting process, similar to Eurocode 8 for determining v_s for a 30-m depth profile.

$$v_{s,50cm} = 0.50 / \Sigma\left(h_i / v_{si}\right) \quad (9)$$

where $v_{s,50cm}$ is the average over 50 cm, h_i (m) is the data interval (typically 1 or 2 cm) and v_{si} is the estimated shear wave velocity from each CPT data interval.

A comparison analysis was performed to evaluate whether four alternative averaging methods result in any differences to the estimated v_s. Figure 6 shows that the choice of method has only a small influence on the final outcome. Since the H&M method is independent of I_c, the first two alternatives give the same result. For a given method, the differences between the results of four alternatives is only about 5 m/s.

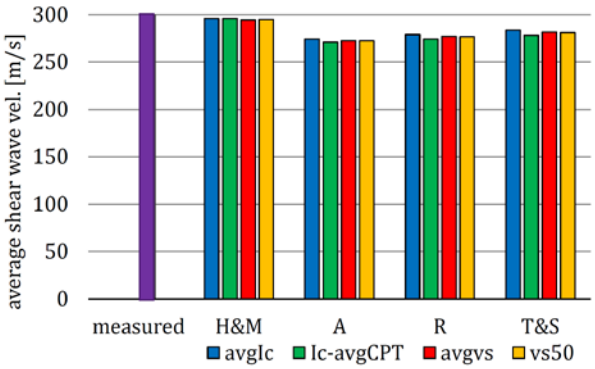

Figure 7. Effect of different averaging schemes

5.4. Predicted v_s from correlations

The best predictions were produced for the group 'a' soils listed above. As shown in Fig. 7, the Robertson, Andrus, and T&S models produced very close predictions with trend slopes almost 1:1 and R^2 values above 0.86. The H&M model predicted less well, over-predicting shear wave velocity consistently.

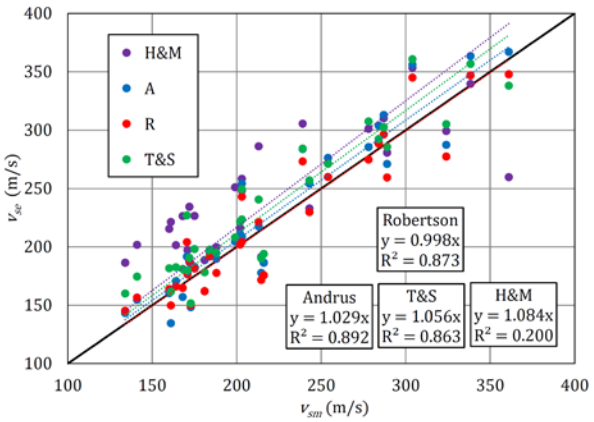

Figure 8. Predictions for soil type (a), Holocene fluvial soils

For the Pleistocene fluvial deposits (b), predictions were more scattered with no discernable correlation by any of the methods. This is perhaps due to high variability of q_c in coarse soils while soil stiffness (ie v_s) does not vary to such a degree.

The Pleistocene aeolian deposits (c) fared better as shown in figure 8. All correlations underpredicted by about 20%. The H&M correlation showed poor R^2 (negative) while the other three had moderate R^2 result (~0.5).

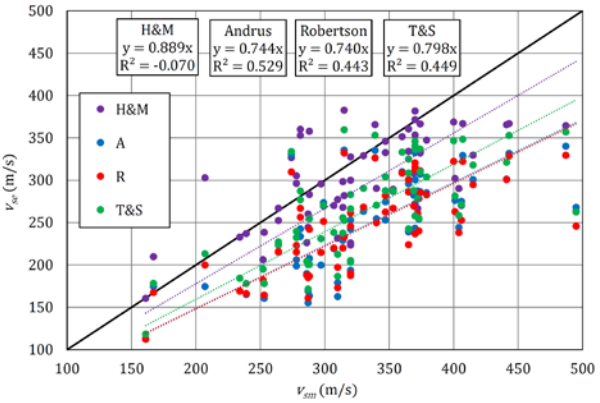

Figure 9. Predictions for soil type (c) Pleistocene aeolian soils

This may be due effects of weak cementation that may be lost during CPT penetration. These soils are the subject of ongoing research at our laboratory.

Tertiary deposits also defied any correlation attempts where again R^2 values were negative for all models.

5.5. Adjusted correlation models

We tried another approach by modifying and fitting the correlation models with our data. The two models we examined were Andrus and Robertson models. The Hegazy and Mayne model did not have a soil type factor, and the Tonni and Simonini model was very similar to the Robertson. For the Andrus model, the correlation equation (Eq. 3) to fit has the form:

$$v_s = a \cdot q_t^{\,b} \cdot I_c^{\,c} \cdot z^d \quad (10)$$

Where a, b, c, and d, are fitting constants. The SF factor was set to one. For the Robertson equation (Eq. 4) we used two varieties:

$$v_s = \left(10^{\alpha_1 \cdot I_c + \beta_1} \cdot \frac{q_t - \sigma_{v0}}{p_a}\right)^{0.5} \quad (11)$$

$$v_s = \left(10^{\alpha_2 \cdot I_c + \beta_2} \cdot \frac{q_t - \sigma_{v0}}{p_a} \right)^{\gamma_2} \quad (12)$$

with $\alpha_1, \beta_1,$ and $\alpha_2, \beta_2, \gamma_2$ being the fitting constants. For each model, the constants were determined by minimizing the sum of the error squared using Solver in Excel.

For the Holocene soils (a) the best fit came from Eq. 11 which is not surprising since the original version also performed well. The correlation was:

$$v_s = 17.66 \cdot q_t^{0.201} \cdot I_c^{0.321} \cdot z^{0.249} \quad (13)$$

with R^2=0.91. The other two correlations produced R^2=0.88.

The Pleistocene fluvial soils (b) improved slightly, with the Robertson correlation performing best (Eq. 12).

$$v_s = 3.25 \cdot q_t^{0.412} \cdot I_c^{0.819} \quad (14)$$

The goodness of fit was still poor (R^2=0.39) but at least it yielded a positive value, compared to negative correlation coefficients in the original assessment. The group a and b soils are shown in Fig. 10.

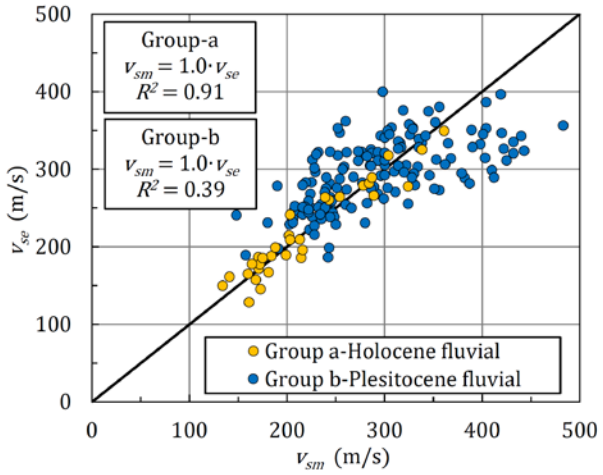

Figure 10. Scatter and correlations for groups a and b soils

For the Pleistocene aeolian soils (c), a noticeable improvement occurred where the underestimation was eliminated from the correlation.

$$v_s = 25.69 \cdot q_t^{0.176} \cdot I_c^{0.713} \cdot z^{0.13} \quad (15)$$

with R^2 = 0.57. The resulting plots are shown in Fig. 11.

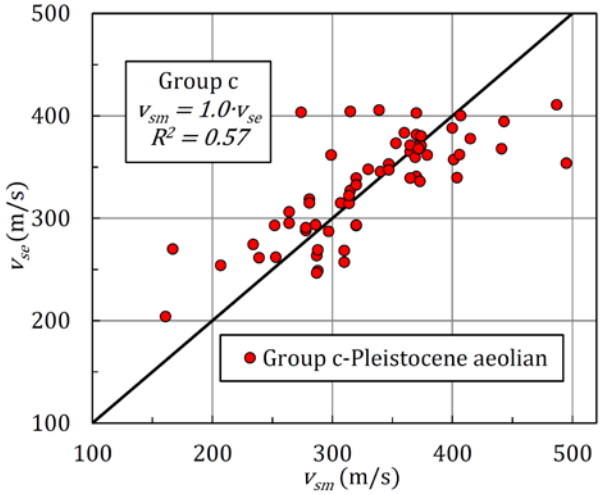

Figure 11. Improved fit for group c soils

Finally, for the tertiary soils from Budapest and Paks-1 sites, we found very little correlation to qc. Instead, v_s was entirely dependent on confining stress. Using this idea as a guide we were able to correlate v_s to depth by:

$$v_s = 91,03 \cdot z^{0.456} \quad (16)$$

where z is depth (m). Of course, this would be difficult to generalize, but for producing useful profiles for site response in these Hungarian soils, the fit is useful (Fig. 12).

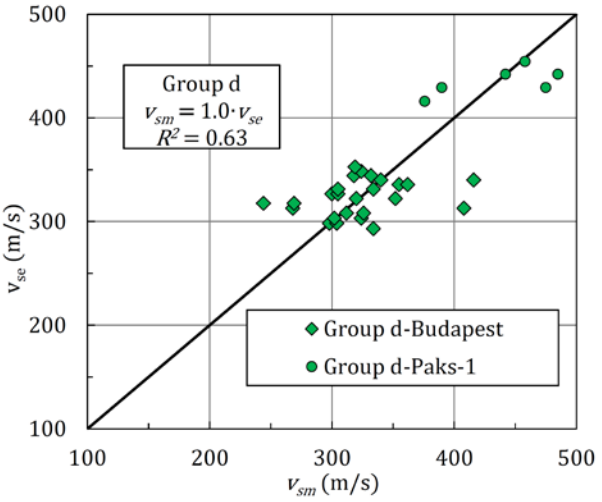

Figure 12. Scatter and correlation for group d soils

6. Field and lab data for response analysis

Several studies are available in the literature concerning ground response analysis, but not many have been performed in the region of the Pannonian Basin where regional seismic risk can be considered moderate. Peak ground acceleration values between 0.08g-0.15g have been determined by seismologists for the usual 10% probability of exceedance in 50 years for the seismic zones given in the Hungarian EC8 National Annex.

To perform ground response analysis for a site, soil profile information must first be gathered; preferably from in-situ measurements and laboratory tests. This information has a strong and direct influence on response analysis results. In this study, we used state-of-the-art soil investigation methods to obtain dynamic soil parameters: shear modulus (G), damping (D) and their variation as a function confining stress and shearing strain level.. Results from different investigation methods have been compared and their effects on ground response analysis results have been determined.

6.1. Exploration

Six CPT's were performed with depths of 18.5-22.0 m. Two of the CPT's included seismic measurements as well. Ten boreholes with similar depths were drilled as well (two 10m, two 20m, and six 25m deep). The shallow boreholes and the top section of all others were drilled dry with 180 mm spiral augers and only disturbed samples were taken. Deeper layers under the quaternary sediments were drilled with a 146 mm diameter hollow stem auger using drilling fluid with continuous sampling.

Later, a more detailed investigation program was performed by the authors aimed at obtaining dynamic soil parameters as discussed in more detail in the following sections. Our program consisted of several MASW profiles, two SCPT soundings, and numerous laboratory measurements using Bender Element (BE) tests, Resonant Column (RC) and Torsional Simple Shear (TOSS) tests.

6.2. MASW and SCPT

Profiles from the MASW and SCPT measurementes were in general agreement. Initially we tried to generate a 2D map of v_s with the MASW array, but low frequency contamination due to traffic noise made this impossible. Two of the profiles are shown in Fig.13 with results from nearby SCPT. Layers are shown as reference to laboratory tests presented later.

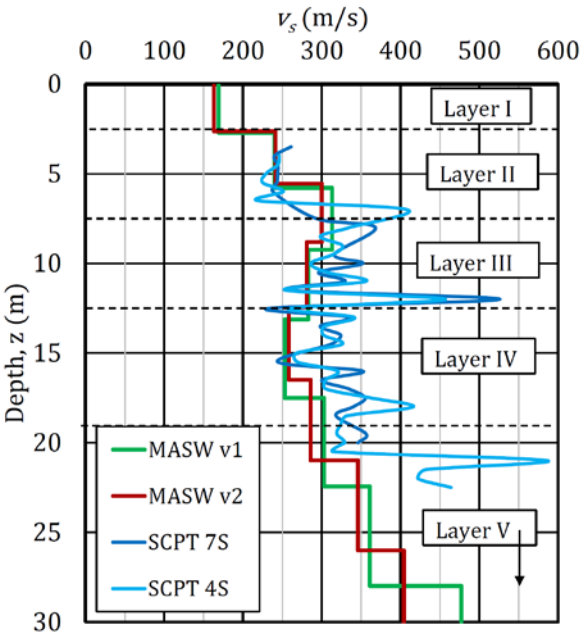

Figure 13. Comparison between MASW and SCPT profiles

To further investigate the correlations between CPT and SCPT, we applied Eq. 4 to a profile and produce fairly good agreement as shown in figure 14.

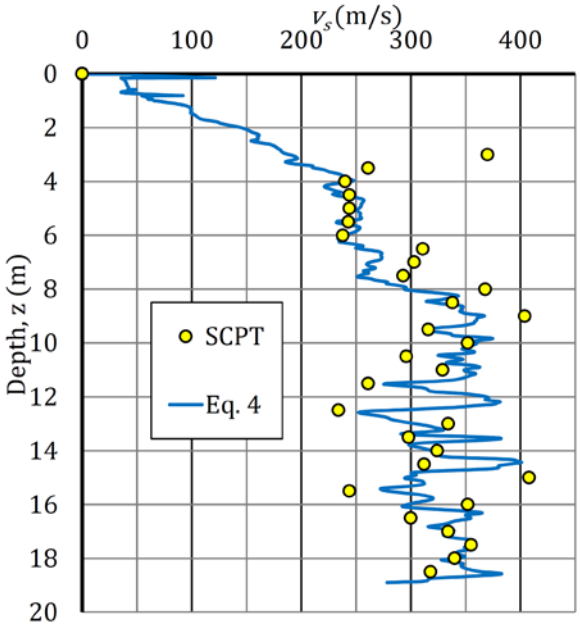

Figure 14. SCPT and CPT estimates for v_s

The two profiles offer a great deal to think about in terms of sampling size, correlations, and the natural variation of soil properties.

6.3. Laboratory testing

A series of bender element (BE), resonant column (RC) and torsional simple shear (TOSS) tests were performed on samples retrieved from the site. Each of these tests offers a different perspective on shear modulus (G), v_s, and damping (D). Effects of confining stress (p,p'), void ratio (e), and shearing strain amplitude (γ) were investigated.

6.3.1. Bender element tests

Samples were confined and saturated to B-values greater than 0.95 then isotropically consolidated in at least four stages. BE measurements were performed periodically and final values of v_s were obtained after primary consolidation. The next consolidation step was applied immediately after primary consolidation as there were time constraints placed on the testing program. Results of the BE tests on all three samples at different confinements are presented in Fig. 15. Fitted curves (with a form similar to Eq.1) are also shown.

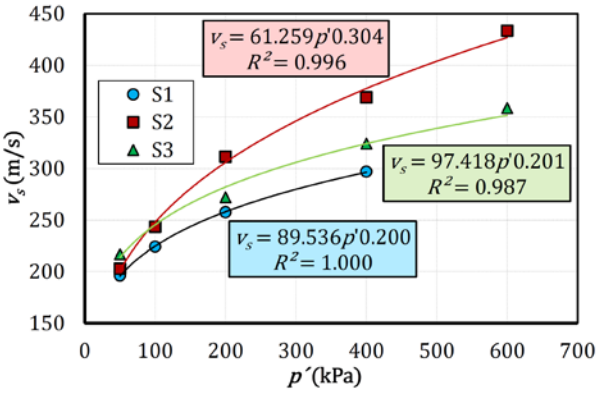

Figure 15. Influence of effective confinement on v_s

It is clear from Fig. 15 that S1 and S3 show a similar trend in evolution of v_s versus p'. More rapid increase in the value of v_s can be observed for confining stresses lower than 200 kPa perhaps because in-situ stresses were higher than that [13]. Higher values of v_s for S3 are mainly caused by its lower void ratio.

It can be seen in Fig. 15 that even though all of the investigated soils from Layer V have similar physical parameters (index of plasticity, degree of saturation and specific density) there is a distinct difference in the evolution of v_s vs p' for S2 and for the other two samples. This could be caused not just by the different void ratios as it will be demonstrated herein, but also by the different values of over-consolidation ratio (OCR), D_{50} (thus clay content) and in-situ state of stress. Based on geological literature, some slight OCR may be expected in Layer V, however measurement of OCR exceeded the scope of this study. Fabric and structure are not expected to play a significant role in this case [14].

Different void ratios (e) were observed across the soil profiles/boreholes on the site for the depths of the tested samples. Thus, it was necessary to obtain a range of values of v_s for different void ratios to incorporate this variation into the ground response calculations. This was done through normalization of G_{max} by a function of void ratio $F(e)$. This function is shown in Eq. 17 and was based on [14].

$$F(e) = (2.973 - e)^2 / (1 + e) \qquad (17)$$

The functional relationships are graphed in Fig. 16. Fitted curves and their constants A and n for obtaining G_{max} can be written in the form:

$$G_{max} = AF(e)p'^{n}. \qquad (18)$$

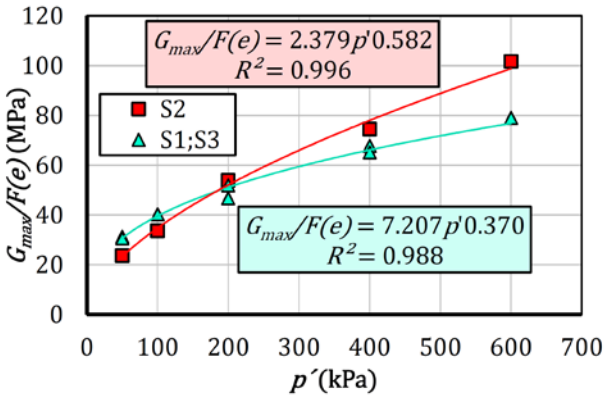

Figure 16. Effect of void ratio and confinement on G_{max}

6.3.2. Resonant column-torsional shear tests

Samples from Layer II and Layer IV were investigated with Resonant Column (RC) and Torsional Simple Shear Testing (TOSS). A combined RC-TOSS device was used for testing which was built then improved [15-18]. The benefit of the combined testing is that not only v_s or G_{max} can be determined as with the other test methods mentioned here, but shear modulus degradation and damping curves can also be obtained.

Samples of the coarse-grained soils of Layer II and Layer IV were obtained with a spiral auger; hence their in-situ state was clearly disturbed. To model their in-situ behavior reconstituted samples were used. State of compaction was estimated based on CPT results and loosest and most dense state was investigated in laboratory. Regular testing sequence consists of (i) RC measurements at lowest strain level for obtaining G_{max}, (ii) assessment of duration of confinement effects with repeated RC measurements (iii) TOSS testing with sine cyclic loading with sequentially increased amplitude to obtain modulus degradation curve, (iv) low strain RC test as control measurement to assess any changes in G_{max} due to TOSS testing. Duration of confinement was found to have no significant effect on v_s after a settling of approx. 30 minutes, during which a 2-3% increase could be observed.

Fig. 17 shows obtained degradation curves compared to often cited curves presented by [19]. Although fines content of tested samples was negligible (1% for S4 and S5, 3% for S6), obtained results seem to fit with curves given for soils with an index of plasticity between 15 - 30 %.

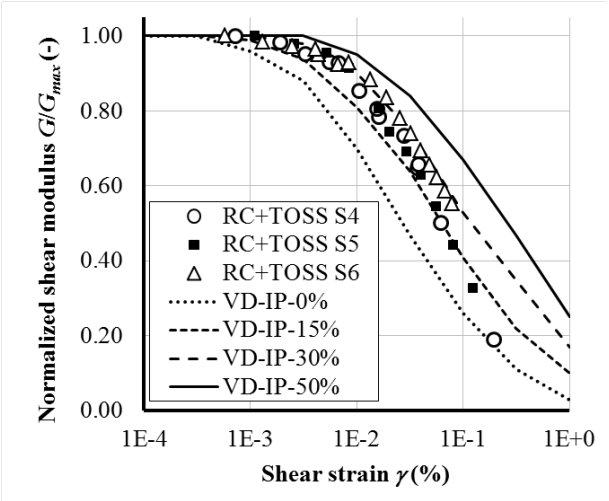

Figure 17. Results of combined RC-TOSS tests.

7. Reconciling field and lab data

As stated in the introduction, the best data will help the engineer make decisions. We wanted to see how to combine the data to produce consistent and reasonable v_s profiles, and apply them to a site response analysis. In doing so, we could construct some typical profiles, evaluate the influence of uncertainty in our analysis, and compare our results to simpler, code-based approaches.

7.1. Combined profiles

Based on field and laboratory measurements, the combined profile is shown in Fig. 18 and it shows a fairly good agreement overall between profiles obtained with MASW and SCPT. In the SCPT profiles a rapid increase in v_s around 12 and 21 m suggest thin layers of gravel which is difficult to detect with MASW. However the deposition of coarse grained materials on the top surface of the Miocene clays around 12m is plausible according to geological descriptions.

Fig 18 shows a very good agreement overall between SCPT measurements and estimated v_s values based on correlations using regular CPT data. A larger scatter in both estimated and measured v_s can be found at locations where there is non-homogeneity of the gravelly sand layers in terms of grain size distribution and especially gravel content.

Shear wave velocity values obtained with BE, RC and TOSS measurements provided a lower bound of the in-situ tests. In terms of BE tests, this may be due to disturbances connected to sampling, transfer of samples and relaxation. Effects of confinement duration may also be a reason behind lower values of v_s. BE tests performed at a confinement corresponding to sample depth are shown with blue triangles. Lower and higher confinement results were used for estimating v_s for regions above and below the sample depth.

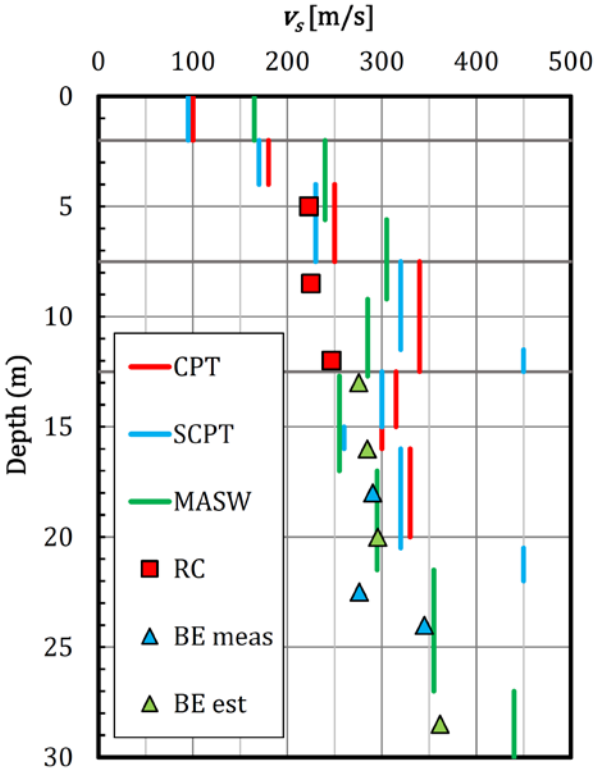

Figure 18. Profiles from all test results

7.2. Profiles for response analysis

Based on the investigations performed with different methods, five 1D models were developed for ground response analysis (Fig. 19). Model A was based on SCPT results. Model B was based on MASW results. Models C and D were obtained using regular CPT data and Robertson correlations (Eq. 4). Model C used the CPT data from the same sounding of a SCPT test and model D included CPT data that revealed a significant presence of the organic Layer III. Model E was based on the laboratory tests (BE, RC, and TOSS).

Additional considerations were necessary for estimating the profile at greater depths. Since there was no clear delineation of "bedrock" at the site, we used some of the p'vs depth relationships found in the laboratory. Modulus reduction curves were also based on laboratory results.

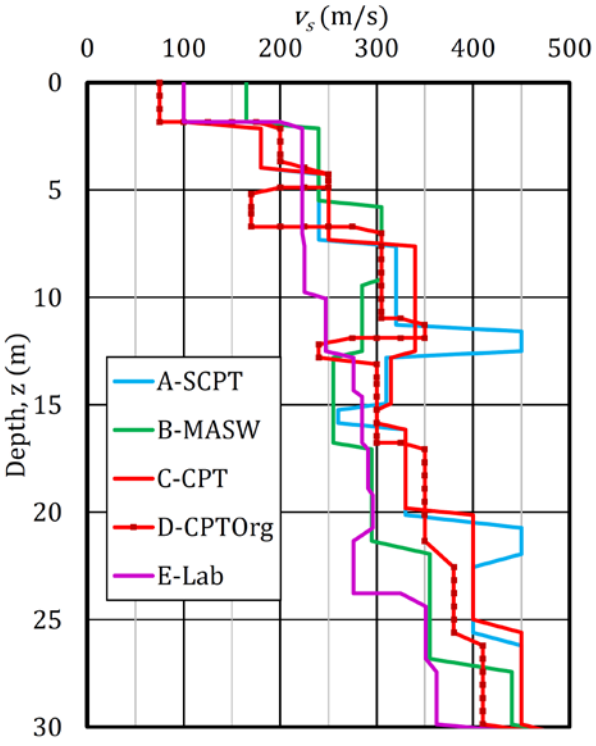

Figure 19. Profiles used in response analysis

The other aspect of profiles we considered was variability. We had some idea about the variablity of v_s on-site as well as with the laboratory results. In order to assess their impact, we varied the profiles as follows:

a) The five models without any variation allowed.
b) Variation of v_s in each layer based on the scatter of the measurements (10 profiles).
c) Variation of layer thickness (10 profiles).
d) Variation of both v_s and layer thickness (50 profiles)
e) Variation of v_s, layer thickness and nonlinear parameters (100 profiles)

The choice of profile depth was also examined since standard practice often uses a simplified 30-m profile designation.

8. 1-D site response analysis

In typical geotechnical engineering practice, v_{s30} has to be assessed for seismic design and in many cases, only the top 30 m of soil layers are investigated. Therefore we performed all calculations with the obtained five models and assuming 30 m as the depth of the bedrock; and we also compared these to calculations with deeper models where we used a power function to estimate deeper layer's v_s based on the measurements done in Layer V. For these runs, depth of bedrock was taken as 110 m based on deep boreholes from the surrounding area and geological descriptions. For all five models, the same evolution of v_s was assumed between 30 m and 110 m. Since in geotechnical engineering practice v_{s30} has to be assessed for seismic design, in many cases only the top 30 m of soil layers are investigated. Therefore we performed all calculations with the obtained five models and assuming 30m as the depth of the bedrock; and we

also compared these to calculations with deeper models where we used a power function to estimate deeper layers' v_s based on the measurements done in Layer V. For these runs, depth of bedrock was taken as 110m based on deep boreholes from the surrounding area and geological descriptions. For all five models, the same evolution of v_s was assumed between 30m and 110m.

One of the main results of this study is shown in Fig. 20 which compares three 30-m deep models based on the different investigation methods. The spectral accelerations represent median values from 7 earthquakes, all scaled to PGA=0.14g. A very good agreement could be found between all spectra obtained with different soil profiles from Fig. 19.

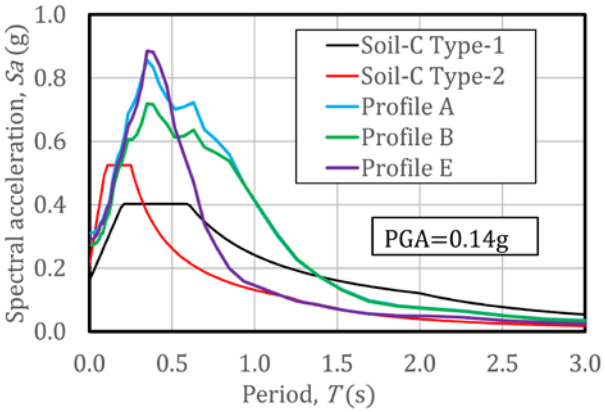

Figure 20. Response spectra from three models

Also shown are the Eurocode spectra for Soil Profile C, Type 1 and 2 scaled to the same PGA. We observed little change in response when extending the profile to 100m depth.

Finally, we tried to assess the effects of uncertainty and variability in our data. A sample of the assessment is shown in Fig. 21 for profile A where v_s and layer thickness were varied based on the variability of our field data. Each of the spectra are median values based on a larege number of random realizations of parameters. In general, varying the parameters reduced amplification. Additionally, the use of a deep (100m) profile shifted the response to longer periods.

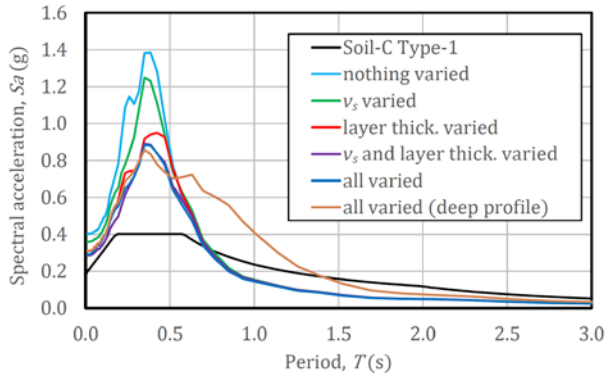

Figure 21. Effect of varying parameters in profile A

Using the same approach for the other profiles B-E produced similar behavior. The interested reader is directed to additional discussion in [20].

9. Conclusions

Our research group has kept a holistic focus to the measurement and analysis of dynamic soil behavior. We have made a purposeful effort to produce practical and immediately applicable results for geotechnical professionals in Hungary. With each new field and laboratory investigation, a final assessment has been made to integrate new knowledge into the overall understanding of dynamic soil behavior. The past ten years have been interesting and rewarding in that we have advanced the level of research and practice to a high level. As with most research and development, many questions remain and many new questions have arisen.

Acknowledgement

This paper was written with the support of the project titled "Internationalisation, initiatives to establish a new source of researchers and graduates and development of knowledge and technological transfer as instruments of intelligent specialisations at Széchenyi István University" (project number: EFOP-3.6.1-16-2016-00017).

References

[1] Sara, MN (1994) Standard Handbook for Solid and Hazardous Waste Facility Assessments, Lewis Publishers ISBN 0-87371-318-4

[2] Kegyes-Brassai, O. (2015): Earthquake Hazard Analysis and Building Vulnerability Assessment to Determine the Seismic Risk of Existing Buildings in an Urban Area, PhD Diss. 199 p

[3] O. Yilmaz., Seismic data processing. Society of Exploration Geophysics, Tulsa, 1987, pp. 62-79.

[4] Park, C. B., Miller, R. D. & Xia, J., 2001. Offset and resolution of Dispersion Curve in Multichannel Analysis of Surface Waves (MASW). Denver, Proceedings of the SAGEEP.

[5] Y. Hegazy and P. Mayne, "Statistical correlations between v_s and cone penetration data for different soil types" *Proceedings, International Symposium on Cone Penetration Testing, CPT '95*, Linkoping, Sweden, Swedish Geotechnical Society, pp. 173-178, 1995

[6] R.D. Andrus, N.P. Mohanan, P. Piratheepan B.S. Ellis and T. L. Holzer, "Predicting shear wave velocity from cone penetration resitance", in *Proceedings, 4th International Conference on Earthquake Geotechnical Engineering, Thessaloniki, Greece, Paper No. 1545, 2007*

[7] P.K. Robertson, "Interpretation of cone penetration tests - a unified approach. *Canadian Geotechnical Journal*, Vol 46. pp. 1337-1355. 2009

[8] L. Tonni and P. Simonini, "Shear wave velocity as function of cone penetration test measurements in sand and silt mixture". Engineering Geology, Vol 163, pp. 55-67 2013.

[9] P.W. Mayne and J.G. Rix, "Correlations between shear wave velocity and cone tip resistance in natural clays," *Soils and Foundations*, JSSMFE, Vol 35(2), pp 107-110, 1995.

[10] Wolf, Á. and Ray, R.P., 2017, April. Comparison and Improvement of the Existing Cone Penetration Test Results–Shear Wave Velocity Correlations for Hungarian Soils. In *Proceedings of ICEES 2017: 19th International Conference on Earthquake Engineering and Seismology*.

[11] C. Madiai and G. Simoni, "Shear wave velocity-penetration resistance correlation for Holocene and Pleistocene soils of an area in central Italy" *Proceedings, 2th International Conference on Geophysical and Geotechnical Site Characterization (ISC'2)*, Rotterdamm, Millpress, pp. 1687-1694, 2004.

[12] T. Ogino, T. Kawaguchi, S. Yamashita, S. Kawajiri. „Measurement deviations for shear wave velocity of bender element test using time domain, cross-correlation, and frequency domain

approaches “, in *Soils and foundations*, Vol. 55, No. 2, Amsterdam: Elsevier B.V., 2015, pp. 329-342.
[13] K. Stokoe, F. Richart, „Shear moduli of soils, in-situ and from laboratory tests.“ *In WCEE, editor, 5th World conference in earthquake engineering*, Rome, Italy, 1973, pp. 356–359.
[14] B.O. Hardin, W. Black, Vibration modulus of normally consolidated clay.“, in *Journal of Soil Mechanics and Foundations Divison*, Vol. 94, No. 2, Reston, VA, ASCE, 1968, pp. 353-369.
[15] R.P. Ray. 1983. *Changes in Shear Modulus and Damping in Cohesionless Soil due to Repeated Loadings*, Ph.D. dissertation, University of Michigan, Ann Arbor, MI., 417 pp.
[16] R.P. Ray, R.D. Woods. 1987. Modulus and Damping Due to Uniform and Variable Cyclic Loading in *Journal of Geotechnical Engineering, Vol. 114, No. 8.* ASCE, pp. 861-876.
[17] R.P. Ray, Z. Szilvágyi, 2013. Measuring and modeling the dynamic behavior of Danube Sands. In Proceedings 18th International Conference on Soil Mechanics and Geotechnical Engineering: Challenging and Innovations in Geotechnics. Paris Presses des Ponts pp. 1575-1578.
[18] Z. Szilvágyi, P. Hudacsek, R.P. Ray, 2016. Soil shear modulus from Resonant Column, Torsional Shear and Bender Element Tests. *In International Journal of Geomate 10:(2)*, pp. 1822-1827.
[19] Vucetic, M. and Dobry, R., 1991. Effect of soil plasticity on cyclic response. *Journal of geotechnical engineering*, *117*(1), pp.89-107.
[20] Szilvágyi, Z., Panuska, J., Kegyes-Brassai, O., Wolf, Á., Tildy, P. and Ray, R.P., 2017. Ground Response Analyses in Budapest Based on Site Investigations and Laboratory Measurements. *Ground Response Analyses in Budapest Based on Site Investigations and Laboratory Measurements, World Academy of Science Engineering and Technology*, pp.307-317.

(1.1)